Journal of Virology®

VIRUS-CELL INTERACTIONS

The Attenuated Pseudorabies Virus Vaccine Strain Bartha Hyperactivates Plasmacytoid Dendritic Cells by Generating Large Amounts of Cell-Free Virus in Infected Epithelial Cells

Jonas L. Delva,[a] Cliff Van Waesberghe,[a] Wim Van Den Broeck,[b] Jochen A. Lamote,[c] Nick Vereecke,[a] Sebastiaan Theuns,[a] Liesbeth Couck,[b] Herman W. Favoreel[a]

[a]Department of Translational Physiology, Infectiology and Public Health, Faculty of Veterinary Medicine, Ghent University, Ghent, Belgium
[b]Department of Morphology, Imaging, Orthopedics, Rehabilitation and Nutrition, Faculty of Veterinary Medicine, Ghent University, Ghent, Belgium
[c]VIB-KULeuven Center for Cancer Biology, VIB FACS Expertise Center, Leuven, Belgium

ABSTRACT Pseudorabies virus (PRV) is a porcine alphaherpesvirus and the causative agent of Aujeszky's disease. Successful eradication campaigns against PRV have largely relied on the use of potent PRV vaccines. The live attenuated Bartha strain, which was produced by serial passaging in cell culture, represents one of the hallmark PRV vaccines. Despite the robust protection elicited by Bartha vaccination, very little is known about the immunogenicity of the Bartha strain. Previously, we showed that Bartha-infected epithelial cells trigger plasmacytoid dendritic cells (pDC) to produce much higher levels of type I interferons than cells infected with wild-type PRV. Here, we show that this Bartha-induced pDC hyperactivation extends to other important cytokines, including interleukin-12/23 (IL-12/23) and tumor necrosis factor alpha (TNF-α) but not IL-6. Moreover, Bartha-induced pDC hyperactivation was found to be due to the strongly increased production of extracellular infectious virus (heavy particles [H-particles]) early in infection of epithelial cells, which correlated with a reduced production of noninfectious light particles (L-particles). The Bartha genome is marked by a large deletion in the US region affecting the genes encoding US7 (gI), US8 (gE), US9, and US2. The deletion of the US2 and gE/gI genes was found to be responsible for the observed increase in extracellular virus production by infected epithelial cells and the resulting increased pDC activation. The deletion of gE/gI also suppressed L-particle production. In conclusion, the deletion of US2 and gE/gI in the genome of the PRV vaccine strain Bartha results in the enhanced production of extracellular infectious virus in infected epithelial cells and concomitantly leads to the hyperactivation of pDC.

IMPORTANCE The pseudorabies virus (PRV) vaccine strain Bartha has been and still is critical in the eradication of PRV in numerous countries. However, little is known about how this vaccine strain interacts with host cells and the host immune system. Here, we report the surprising observation that Bartha-infected epithelial porcine cells rapidly produce increased amounts of extracellular infectious virus compared to wild-type PRV-infected cells, which in turn potently stimulate porcine plasmacytoid dendritic cells (pDC). We found that this phenotype depends on the deletion of the genes encoding US2 and gE/gI. We also found that Bartha-infected cells secrete fewer pDC-inhibiting light particles (L-particles), which appears to be caused mainly by the deletion of the genes encoding gE/gI. These data generate novel insights into the interaction of the successful Bartha vaccine with epithelial cells and pDC and may therefore contribute to the development of vaccines against other (alpha-herpes)viruses.

KEYWORDS suid herpesvirus 1, Aujeszky's disease virus, pseudorabies virus, PRV, Bartha, Bartha-K61, plasmacytoid dendritic cells, glycoprotein E, glycoprotein I, US2, interferon, plasmacytoid dendritic cell, gE/gI, pDC

Editor Felicia Goodrum, University of Arizona

Address correspondence to Herman W. Favoreel, herman.favoreel@ugent.be.

The authors declare no conflict of interest.

Received 23 December 2021
Accepted 27 April 2022
Published 23 May 2022

Suid herpesvirus 1, Aujeszky's disease virus, or pseudorabies virus (PRV) is a prototypical alphaherpesvirus and the causative agent of Aujeszky's disease (1). In pigs, PRV infections manifest as respiratory, neurological, and/or reproductive illness depending on the age of the pig, while in other susceptible hosts, infection causes severe neurological symptoms and is invariably lethal (1, 2). Because of the catastrophic impact of PRV outbreaks on pig industries (3), tremendous efforts have been made to develop vaccines and eradication programs against PRV (4). One of the gold-standard PRV vaccines is the attenuated Bartha-K61 strain (5, 6). Although its origin is uncertain, it was made by serial passaging, which led to the incorporation of various mutations into the viral genome (7). The Bartha strain displays a variety of mutations scattered over the entire length of the genome (7–11), but it is marked particularly by a large 3.4-kbp deletion in the unique short (US) region of the genome, affecting the genes encoding US7 (glycoprotein I [gI]), US8 (gE), US9, and US2 (12). The membrane proteins gE and gI function as a heterodimer (13) in conjunction with US9 in anterograde neuronal transport (14–21). In addition, the gE/gI heterodimer is also involved in viral protein sorting, cell-to-cell spread, and plaque formation (21–24). In line with this, the Bartha strain produces smaller plaques upon infection in cell monolayers than wild-type (WT) PRV strains (25). More recently, we demonstrated that gE suppresses type I interferon (IFN) production by plasmacytoid dendritic cells (pDC) in response to PRV-infected cells (26). US2, on the other hand, is a small, prenylated viral tegument protein that associates with the plasma membrane of the infected cell. It binds the cellular extracellular signal-regulated kinase 1/2 (ERK1/2) kinase and sequesters it at the plasma membrane (27–30). While gE and gI play important roles as virulence factors *in vivo* in different infection models (14, 31, 32), the role of US2 during viral pathogenesis in animals is less clear (32, 33).

pDC constitute a small subset of peripheral blood mononuclear cells (PBMC), representing only 0.1 to 0.5% of the total cell population, yet they can produce up to 1,000 times more type I IFNs than any other cell type (34, 35). Not surprisingly, they are considered major if not the sole producers of type I IFNs in the PBMC population upon alphaherpesvirus infections, including herpes simplex virus 1 (HSV-1) and PRV (36, 37). Given that pDC may also produce other proinflammatory cytokines such as interleukin-12 (IL-12), IL-6, and tumor necrosis factor alpha (TNF-α), they play an important role in shaping the immune response against and the control of alphaherpesvirus infections (38–46). Previously, we reported that type I IFN production by pDC in response to PRV strictly depends on the presence of extracellular virions (or H-particles), while so-called virus light particles (L-particles) that lack DNA and capsid suppress this pDC response (37). Moreover, we also found that epithelial cells infected with the PRV vaccine strain Bartha trigger strongly increased type I IFN production by pDC compared to cells infected with WT PRV (26).

In this study, we report that the hyperactivation of pDC in response to Bartha-infected epithelial cells stretches beyond the production of massive amounts of IFN-α and also leads to the production of large amounts of IL-12/23 and TNF-α but not IL-6. Moreover, we found that epithelial cells infected with Bartha PRV show an increased rate of production of extracellular infectious virus (and reduced production of L-particles) compared to WT PRV and that this correlates with the increased IFN-α response by pDC elicited by Bartha. Importantly, using single-gene-deletion mutants, we show that the deletion of US2 or gE/gI increases the production of extracellular infectious virus and concomitantly leads to the increased activation of pDC, whereas the deletion of gE/gI significantly reduces the production of L-particles in infected epithelial cells.

RESULTS

PRV Bartha-infected epithelial cells induce hyperactivation of pDC cytokine production. Previously, we demonstrated that porcine pDC mount a vigorously increased IFN-α response when incubated with porcine swine testis (ST) cells infected with the PRV vaccine strain Bartha compared to ST cells infected with wild-type (WT) PRV, which was partially caused by the deletion of the gE/gI genes in the Bartha genome (26). As a first step to further characterize this phenotype, we investigated the

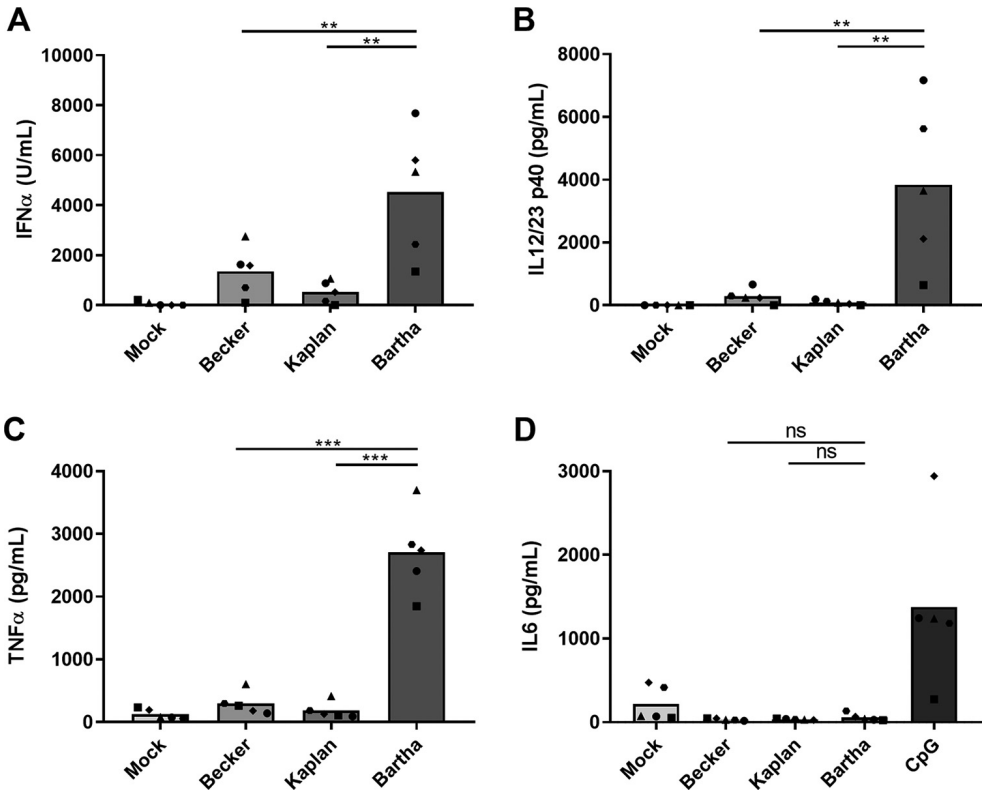

FIG 1 Bartha-infected cells trigger elevated cytokine responses in pDC compared to cells infected with WT PRV. Confluent ST cells were mock inoculated or inoculated with WT Becker, WT Kaplan, or Bartha PRV (MOI of 10) for 2 h, after which the cells were washed and coincubated with pDC-enriched PBMC populations. The supernatant was collected 22 h later and analyzed by ELISAs, quantifying IFN-α (A), IL-12/23 p40 (B), TNF-α (C), and IL-6 (D). For the latter, as a positive control, pDC-enriched PBMC populations were also stimulated with CpG ODN (ns, not significant; **, $P < 0.01$; ***, $P < 0.001$).

effect of Bartha-infected ST cells on the production of other important cytokines by pDC, specifically IL-6, TNF-α, and IL-12/23. Figure 1 shows that pDC-enriched PBMC populations incubated with Bartha-infected ST cells produce strongly increased amounts of both TNF-α and IL-12/23 compared to pDC incubated with cells infected with WT PRV strain Kaplan or Becker. Interestingly, no increased production of IL-6 was observed, whereas the positive control for pDC activation via double-stranded DNA, the Toll-like receptor 9 (TLR9) ligand CpG ODN D32, triggered marked IL-6 production, as expected (Fig. 1D).

To assess whether the measured cytokines indeed originated from pDC in the pDC-enriched PBMC populations, ST cells infected with PRV (Bartha or WT) were incubated with (i) pDC-enriched PBMC populations, (ii) the corresponding amounts of fluorescence-activated cell sorting (FACS)-purified pDC, or (iii) PBMC populations in which the pDC subpopulation was FACS depleted. As an additional control, to assess whether infected ST cells themselves produce detectable amounts of the measured cytokines, PRV-infected ST cells alone, without the addition of any PBMC type, were also analyzed. As negative and positive stimulation controls, mock-infected ST cells and the TLR9 ligand CpG ODN D32 were used, respectively. Figure 2 demonstrates that FACS-sorted pDC and pDC-enriched PBMC (containing the corresponding amounts of pDC) displayed nearly identical IFN-α, IL-12/23a, and TNF-α responses upon stimulation with PRV-infected ST cells or with CpG. In line with this, the production of these cytokines was nearly undetectable when pDC were stimulated with mock-infected/mock-treated ST cells and under conditions without pDC, i.e., ST cells alone or pDC-depleted PBMC. These data demonstrate that pDC are the main producers of IFN-α, TNF-α, and IL-12/23 in these cell populations in response to PRV.

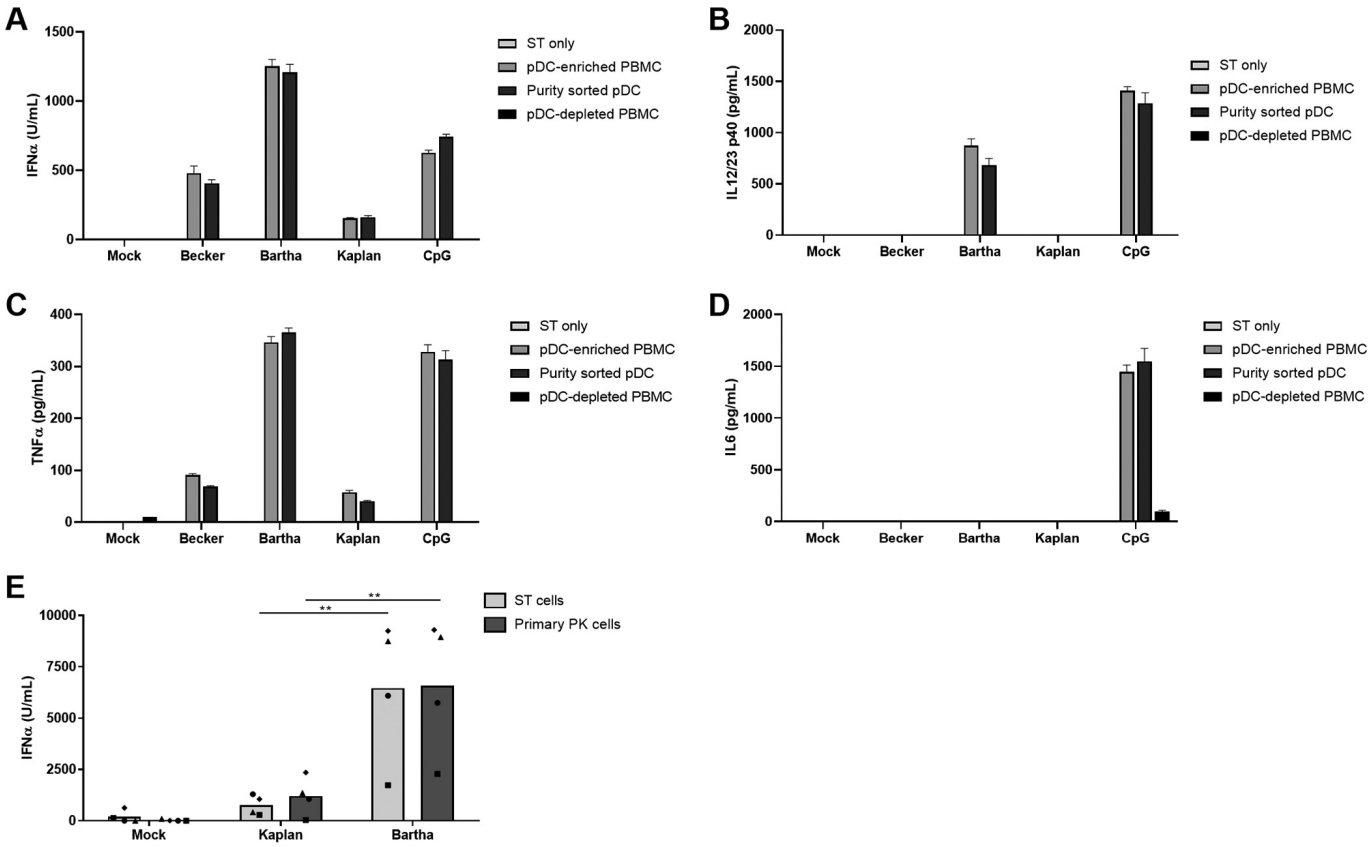

FIG 2 Hyperactivation of pDC induced by Bartha-infected ST cells does not depend on other PBMC subpopulations and is also observed using infected primary epithelial cells. (A to D) Confluent ST cells were mock inoculated or inoculated with WT Becker, WT Kaplan, or Bartha PRV (MOI of 10) for 2 h, after which the cells were washed and overlaid with pDC medium only or pDC medium containing pDC-enriched PMBC, FACS-sorted pDC, or FACS-pDC-depleted PBMC populations. As a positive control, pDC were stimulated with CpG ODN. The supernatant was collected 22 h later and analyzed by ELISAs, quantifying IFN-α (A), IL-12/23 p40 (B), TNF-α (C), and IL-6 (D). Error bars represent the standard deviations from two technical replicates. (E) Confluent primary PK cells or ST cells were mock inoculated or inoculated with WT Kaplan or Bartha PRV (MOI of 10), followed by the removal of the inoculum at 2 hpi and the addition of pDC-enriched PBMC for another 22 h. IFN-α concentrations were determined by an ELISA (**, $P < 0.01$).

To confirm that the hyperactivating effect of Bartha-infected epithelial cells on pDC is not due to the use of immortalized epithelial cells (ST cells), primary porcine kidney (PK) cells were used. Figure 2E shows that, like for ST cells, the incubation of PRV Bartha-infected primary PK cells with pDC-enriched PBMC triggered a significantly increased IFN-α response compared to that using WT PRV Kaplan-infected PK cells (Fig. 2E).

Overall, these data show that epithelial cells infected with the PRV Bartha vaccine strain trigger hyperactivation of pDC, resulting in the massively increased production of IFN-α, TNF-α, and IL-12/23, and that pDC are major producers of these cytokines in PBMC stimulated with PRV-infected cells.

Bartha PRV rapidly reaches high viral titers early during infection of epithelial cells compared to WT PRV. We previously demonstrated that DNA-containing PRV virions are necessary for pDC activation in response to PRV (37). Since pDC show an increased IFN response upon contact with Bartha-infected cells compared to WT PRV-infected cells, one-step growth analyses were performed to assess whether the kinetics of infectious virus production in Bartha-infected cells were different from those in cells infected with the WT PRV strain Kaplan. Figure 3A shows that early in infection, the production of extracellular infectious virus in Bartha-infected cells increases more rapidly than that in WT PRV-infected cells, with over 1,000-fold increased production of extracellular infectious virus at the early time point of 6 h postinoculation (hpi). The extracellular infectious titer of Bartha-infected cells remains significantly increased at later time points (8 hpi, 10 hpi, and 12 hpi) but from 16 hpi onward reaches a plateau similar to that observed for WT PRV-infected cells. Interestingly, the intracellular virus titers (Fig. 3B) of Bartha-infected ST cells did not show the same pattern as that of the

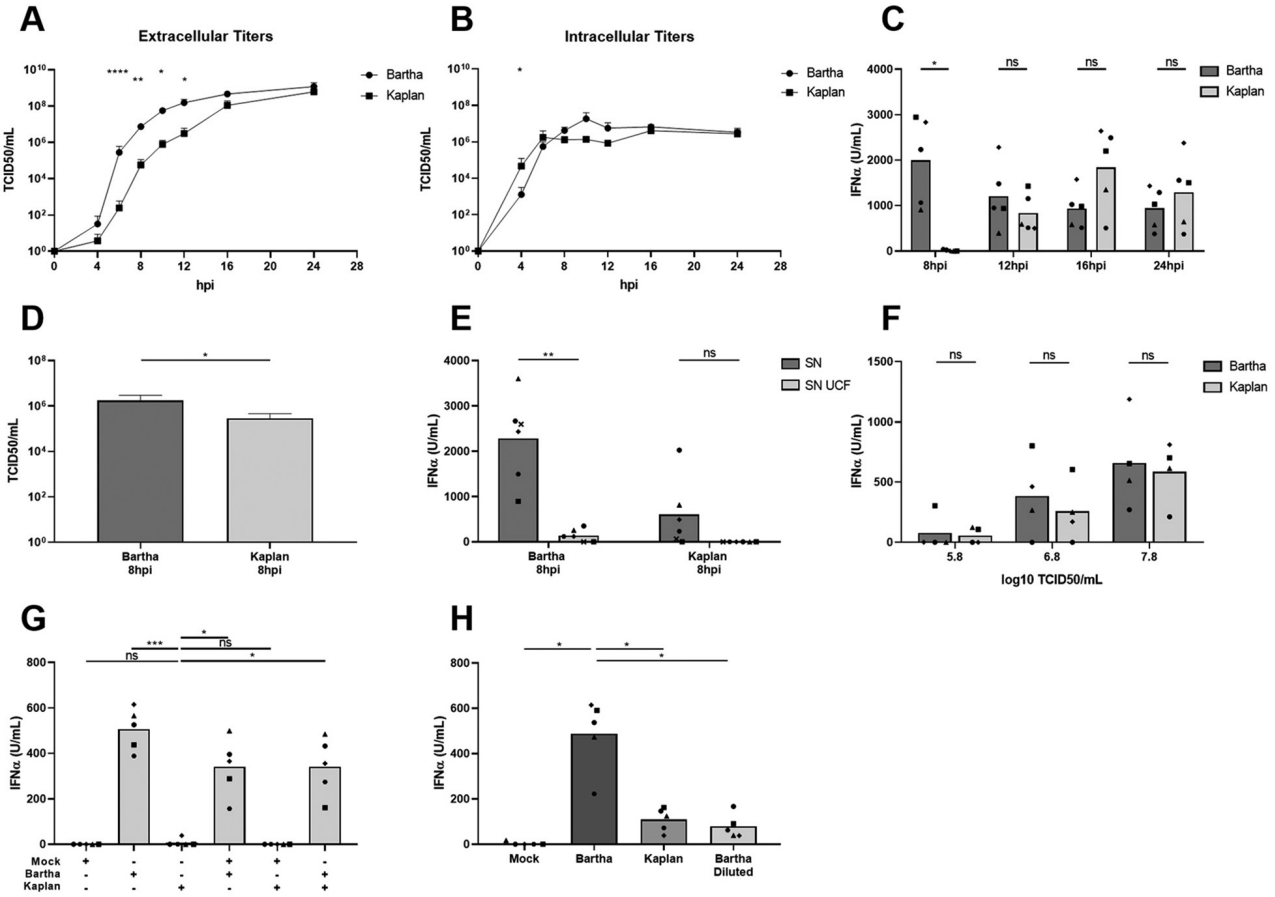

FIG 3 Bartha PRV-infected epithelial cells display increased virus growth kinetics, which leads to an increased IFN-α response by pDC. (A and B) Confluent ST cells were inoculated with WT Kaplan or Bartha PRV (MOI of 10), followed by the removal of the inoculum at 2 hpi and a low-pH treatment to inactivate the remaining inoculum virus. Next, cells were overlaid with ST medium, and the supernatants and infected cells were collected at several time points postinfection. Prior to cell harvesting, infected cells were treated with citrate buffer to inactivate any extracellular cell-adherent virus. Extracellular (A) and intracellular (B) viral titers shown represent average values $\pm$ standard deviations from three independent repeats. (C) Confluent ST cells were inoculated with WT Kaplan or Bartha PRV (MOI of 10) for 2 h, after which the cells were washed and overlaid with pDC medium. The supernatant was collected at 8 hpi, 12 hpi, 16 hpi, and 24 hpi and added to pDC-enriched PBMC populations for 22 h, after which IFN-α production was measured via an ELISA. (D) Confluent primary PK cells were inoculated with WT Kaplan or Bartha PRV (MOI of 10) for 2 h, after which the cells were washed and overlaid with pDC medium. The supernatant was collected at 8 hpi and titrated. Viral titers shown represent average values $\pm$ standard deviations from four independent repeats. (E) Confluent ST cells were inoculated with WT Kaplan or Bartha PRV (MOI of 10) for 2 h, after which the cells were washed and overlaid with pDC medium. The supernatant (SN) was collected at 8 hpi and subjected or not to ultracentrifugation (UCF) to remove virions. Next, the supernatant was added to pDC-enriched PBMC for 22 h, after which the IFN-α concentration was determined via an ELISA. (F) Confluent ST cells were inoculated with WT Kaplan or Bartha PRV (MOI of 10) for 2 h, after which the cells were washed and overlaid with ST medium. At 24 hpi, the supernatants were collected, and infectious virions were purified using linear density gradient ultracentrifugation. Normalized virion titers were subsequently added to pDC-enriched PBMC for 22 h, and IFN-α titers were determined via an ELISA. (G) Confluent ST cells were mock inoculated or inoculated with WT Kaplan or Bartha PRV (MOI of 10) for 2 h, after which the cells were washed and overlaid with pDC medium. The supernatant was collected at 8 hpi and mixed 1:1 as indicated by "+." The obtained supernatant combinations were then added to pDC-enriched PBMC for 22 h, and IFN-α titers were determined via an ELISA. (H) Confluent ST cells were mock inoculated or inoculated with WT Kaplan or Bartha PRV (MOI of 10) for 2 h, after which the cells were washed and overlaid with pDC medium. The supernatant was collected at 8 hpi and titrated. The Bartha supernatant was diluted with pDC medium to equalize the lower Kaplan titer. The obtained supernatants were used to stimulate pDC-enriched PBMC for 22 h, and IFN-α titers were determined via an ELISA (ns, not significant; *, $P < 0.05$; **, $P < 0.01$; ***, $P < 0.001$; ****, $P < 0.0001$).

extracellular virus titers. Indeed, very early in infection (4 hpi), the intracellular virus titer in Bartha-infected ST cells is significantly lower than that observed in WT PRV-infected cells. At later time points, the intracellular virus titers of Bartha-infected cells catch up with (6 hpi) and even exceed (8 hpi, 12 hpi, and 16 hpi), albeit nonsignificantly, those of WT PRV-infected cells.

To assess whether the elevated viral titers in the supernatant of Bartha-infected cells early in infection may explain the hyperactivating effect of Bartha-infected cells on pDC, the supernatant from Bartha- or WT PRV Kaplan-infected cells was collected at 8 hpi, 12 hpi, 16 hpi, and 24 hpi and added to pDC-enriched PBMC. Here, we observed that, specifically, the supernatant collected at 8 hpi from Bartha-infected cells shows a strongly

increased pDC IFN-α response compared to that of Kaplan-infected cells, whereas the supernatants collected at later time points have a roughly similar capacity to trigger interferon production by pDC (Fig. 3C). Importantly, as can be seen in Fig. 3D, Bartha PRV extracellular virus titers at 8 hpi are also higher in primary PK cells, again indicating that this phenotype is not caused by the use of immortalized epithelial cells. To exclude any potential effects caused by other factors in the Bartha supernatant, in particular cytokines, the supernatant of infected ST cells collected at 8 hpi was depleted of PRV virions by ultracentrifugation and used to stimulate pDC. Figure 3E shows that the removal of PRV virions virtually abolishes the IFN-α response, supporting that the viral particles in the supernatants of both Bartha- and WT PRV-infected cells are required for the stimulation of pDC, which is in line with previous observations (37).

Previous research has shown that Bartha virions have an altered virion composition compared to WT strains (6–12), including the absence of gE. To assess whether the differences in virion composition between Bartha and WT PRV may result in differences in pDC activation, the pDC-stimulating potencies of equal numbers of purified Bartha and WT PRV virions were compared. Therefore, Bartha and Kaplan virions (so-called heavy particles [H-particles]) were isolated via linear density ultracentrifugation and added to pDC-enriched PBMC at several infectious titers. Figure 3F shows that regardless of the viral titer, purified Bartha and Kaplan virions induce nearly identical IFN-α responses in pDC, implying that the altered virion architecture of Bartha virions does not contribute significantly to the augmented pDC IFN-α response triggered by Bartha-infected cells.

Although these results suggest that the Bartha supernatant at 8 hpi is more stimulatory for pDC than the WT supernatant because of increased virus titers, this does not formally exclude the possibility that the supernatant from WT PRV-infected cells may poorly stimulate pDC due to the presence of inhibitory factors. To further address this, we mixed the supernatant of Bartha-infected cells collected at 8 hpi with the supernatant from WT PRV-infected cells (also at 8 hpi) or from mock-infected cells. Figure 3G shows that a 1:1 mixture of the supernatant derived from Bartha-infected cells with either the mock supernatant or the supernatant derived from WT PRV-infected cells only slightly reduces the pDC IFN-α response compared to the supernatant derived from Bartha-infected cells. To further strengthen these observations, we subsequently diluted the supernatant of Bartha-infected ST cells collected at 8 hpi down to the virus titer of the supernatant of WT PRV-infected cells and used this to stimulate pDC. This assay demonstrated that the amounts of IFN-α produced by pDC in response to the diluted Bartha supernatant and the undiluted Kaplan supernatant, which contain equal virus titers, are similar (Fig. 3H).

In conclusion, these data support the idea that Bartha-infected epithelial cells hyperactivate pDC due to the faster production of extracellular infectious virus in Bartha-infected porcine epithelial cells than in cells infected with WT PRV.

Bartha-infected epithelial cells do not display increased production of structural components or viral genomes but produce fewer L-particles. Our data demonstrate that the production of extracellular infectious virus occurs more rapidly in Bartha-infected cells than in cells infected with WT PRV. This may be counterintuitive at first sight since the Bartha vaccine strain is an attenuated virus strain, characterized by a drastically reduced cytopathic effect, a small-plaque phenotype on epithelial monolayers (in part due to the deletion of the glycoprotein gE), and severely reduced virulence *in vivo* (5, 6). Seeing the somewhat surprising nature of our results in this context, we sought to confirm the archetypal Bartha small-plaque phenotype compared to WT PRV strains. Plaque sizes were analyzed on confluent ST monolayers overlaid with medium containing carboxymethyl cellulose to prevent secondary plaque formation. Comparison with the two WT PRV strains Becker and Kaplan confirmed that Bartha indeed shows a significantly reduced efficiency in plaque formation (Fig. 4A), in line with previous data (5, 25). Furthermore, flow cytometric analysis demonstrated that Bartha-infected cells express the viral glycoprotein gB but not the viral glycoprotein gE (Fig. 4B), again in line with previous data (47).

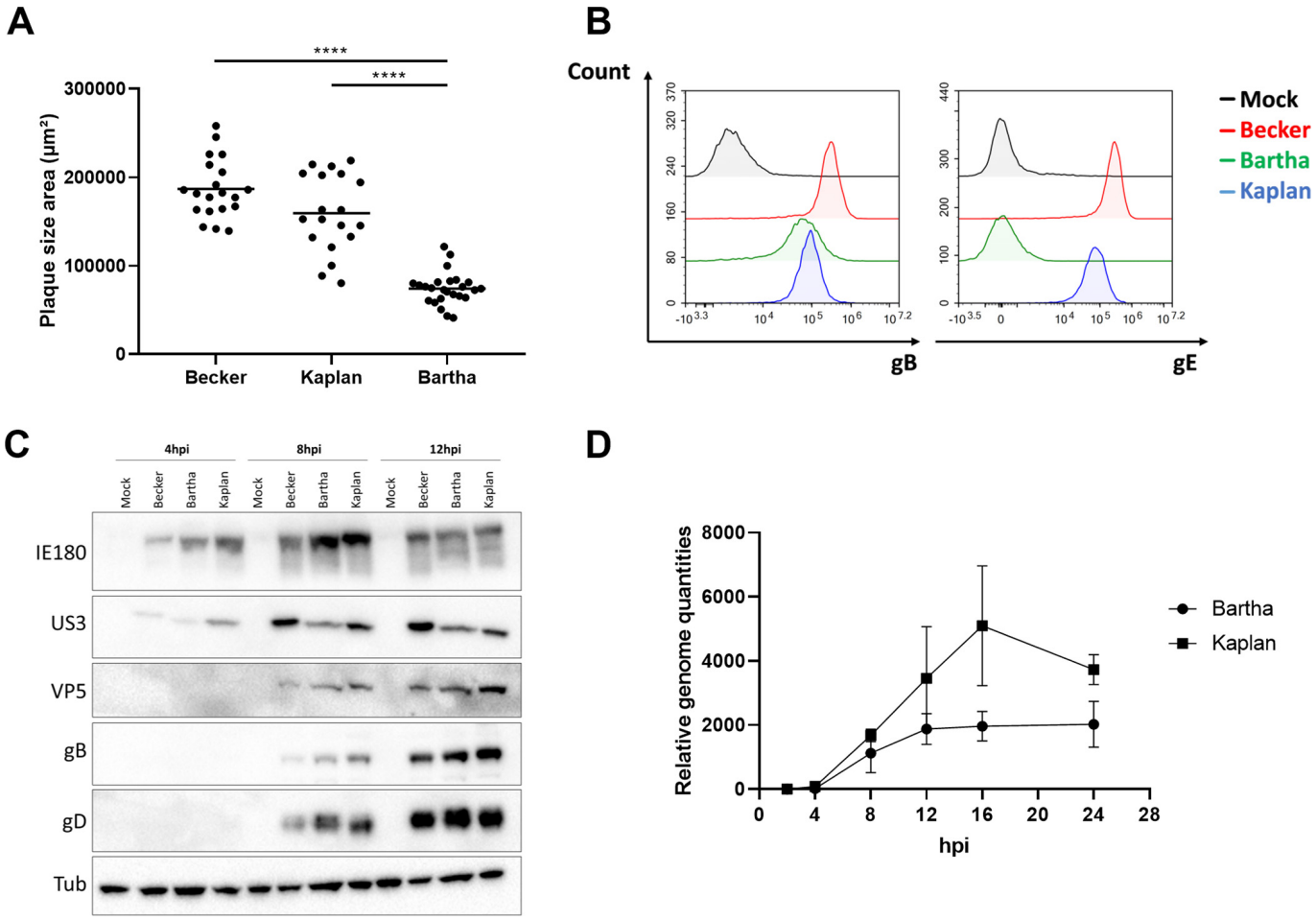

FIG 4 Bartha PRV displays protein expression kinetics similar to those of WT PRV and slightly reduced genome replication in ST cells. (A) Plaque sizes of confluent ST cells infected with WT Becker, WT Kaplan, or Bartha PRV (MOI of 0.001) at 24 hpi. (B) Flow cytometric analysis of ST cells that were mock inoculated or inoculated with WT Becker, WT Kaplan, or Bartha PRV (MOI of 10) and analyzed at 24 hpi for the expression of glycoproteins gB and gE. (C) Western blot analysis of ST cells that were mock inoculated or inoculated with WT Becker, WT Kaplan, or Bartha PRV (MOI of 10) and analyzed at 4, 8, and 12 hpi for the expression of different (viral) proteins. Tub, tubulin. (D) ST cells were inoculated with WT Kaplan or Bartha PRV (MOI of 10) for 2 h, after which the cells were washed and overlaid with ST medium. Cells were collected at 4, 8, and 12 hpi, and DNA was isolated and quantified via qPCR. The normalized genome copy numbers shown represent average values ± standard deviations from three independent repeats (****, $P < 0.0001$).

In order for virions to assemble, structural viral proteins have to be produced in the infected cells. To assess any potential differences in (structural) protein production in cells infected with either Bartha or the WT PRV strain Kaplan or Becker, the production of the immediate early protein IE180, the early protein US3, and the late proteins VP5, gB, and gD was examined via Western blotting at 4 hpi, 8 hpi, and 12 hpi. Despite the observed rapid increase in viral titers, no augmented production of any of these viral proteins could be observed in Bartha-infected cells (Fig. 4C).

Since Bartha infectious virus production occurs more rapidly without increased viral protein expression, we wondered whether Bartha genomes are produced faster in infected cells than WT PRV, as this possibly would allow more nucleocapsids to assemble in the cell nucleus. PRV genome copy numbers were determined via quantitative PCR (qPCR) in a time course experiment in infected ST cells (Fig. 4D). Again, in contrast to the viral titers, Bartha genome replication kinetics were not increased (and, in fact, showed a nonsignificant decrease) compared to those of the WT PRV strain Kaplan. In conclusion, these data show that the faster production of infectious virus of the PRV strain Bartha is not caused by differences in the production of viral structural proteins or viral genome replication.

Even though Bartha-infected cells are not more rapid in the production of structural viral proteins or the replication of viral genomes, infectious H-particles are produced

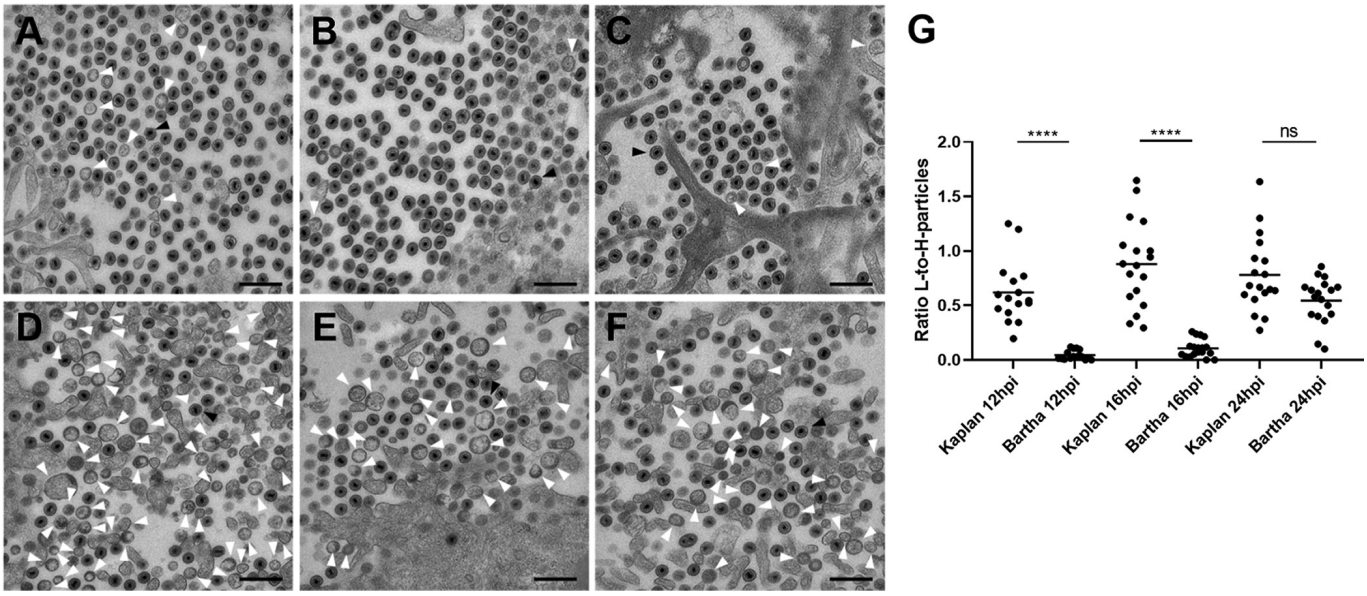

FIG 5 Bartha-infected ST cells produce fewer noninfectious L-particles at 12 hpi and 16 hpi. (A to F) Transmission electron microscopy analysis of ST cells infected with Bartha PRV (A to C) or WT Kaplan PRV (D to F) at 12 hpi. White arrowheads indicate several L-particles (lacking a nucleocapsid), and black arrowheads indicate an exemplary H-particle. Bars, 500 nm. (G) Quantification of the L-to-H-particle ratio for Kaplan- and Bartha-infected ST cells analyzed at 12 hpi, 16 hpi, and 24 hpi (ns, not significant; ****, $P < 0.0001$).

more rapidly. Based on this information, we hypothesized that perhaps in Bartha infected cells, H-particle assembly occurs more efficiently. To explore this, ST cells infected with Bartha or WT PRV at 12 hpi were analyzed by transmission electron microscopy (TEM) (Fig. 5A to F). Strikingly, we noted a clear difference in the presence of secreted light particles (L-particles) between Bartha-infected and WT PRV-infected cells. L-particles are noninfectious virus-like particles that lack a nucleocapsid and are produced by all alphaherpesviruses studied thus far (48). Bartha-infected cells produced almost no secreted L-particles, even though plentiful H-particles could be distinguished (Fig. 5A to C). In contrast, WT PRV-infected cells produced very substantial amounts of both L-particles and H-particles (Fig. 5D to F).

To assess this in more detail, L- and H-particle production by Bartha and WT PRV-infected ST cells was assessed at different time points. Figure 5G shows that in addition to 12 hpi, very few L-particles are produced by Bartha-infected cells at 16 hpi, again in contrast to WT PRV-infected cells. At 24 hpi, Bartha-infected cells produce L-particles albeit at levels still somewhat, but nonsignificantly, reduced compared to those of WT PRV-infected cells.

These observations suggest a model of the more efficient assembly and egress of infectious virions in Bartha PRV-infected cells, as fewer structural viral proteins appear to be used for noninfectious L-particle formation.

Increased infectious virus production in Bartha-infected epithelial cells is caused by deletion of the US2 and gE/gI genes. One of the most prominent alterations in the Bartha genome compared to WT PRV strains is the deletion of a 3.4-kb sequence in the unique short (US) region encompassing the US7 (gI), US8 (gE), US9, and US2 genes. Of interest, another attenuated PRV vaccine strain that was generated by serial passaging (49, 50), the BUK strain, has a similar deletion in the US region of the genome, encompassing the genes encoding gE, US9, and US2 (47, 51). This prompted us to investigate whether the BUK strain similarly displays increased extracellular titers early in infection of ST cells. Figure 6A shows that, indeed, BUK extracellular titers at 8 hpi are significantly increased compared to those of both Becker and Kaplan WT PRVs. Correspondingly, this also led to an increased IFN-α response by pDC (Fig. 6B). These observations strongly suggest that the genes affected by the large US deletions in both the Bartha and BUK genomes, i.e., gE/gI, US9, and/or US2, are responsible for the observed increased extracellular viral titers early in infection.

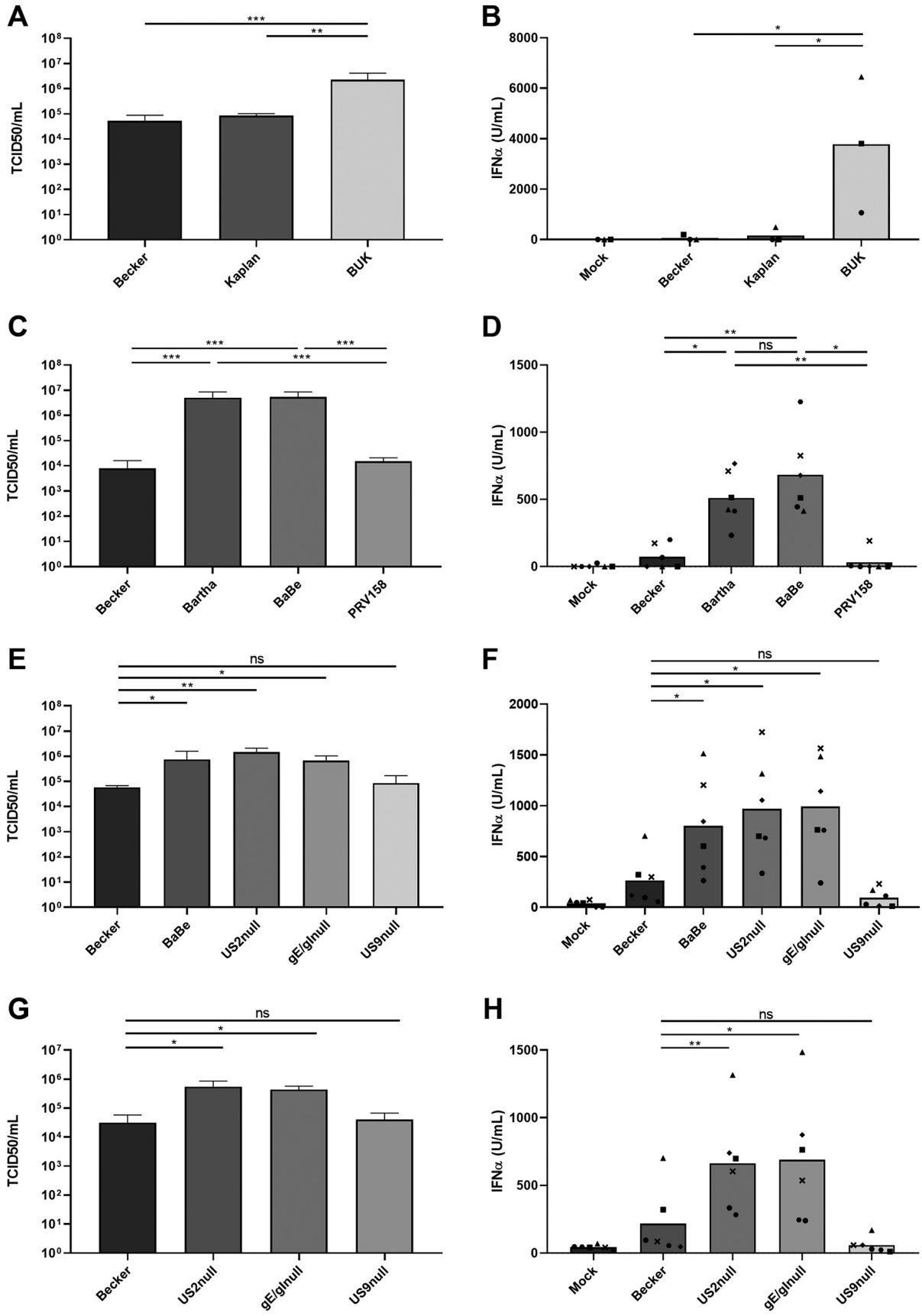

FIG 6 Deletion of the PRV genes US2 and US7/US8 results in increased extracellular virus titers in infected epithelial cells and a correspondingly increased IFN-α response by pDC. (A to F) Confluent ST cells were mock inoculated or inoculated with different PRV

(Continued on next page)

To further investigate if the US deletion in the Bartha genome is critical for the observed increase in the virus titer (and, consequently, increased pDC activation), ST cells were mock infected or infected with WT PRV strain Becker, PRV strain Bartha, or the isogenic strain PRV158 (Bartha strain with the large US deletion repaired using the corresponding WT Becker strain sequence) or BaBe (WT Becker strain with the same large US deletion as that present in Bartha). Figure 6C shows that infectious virus titers at 8 hpi of ST cells infected with BaBe were significantly higher than those observed using WT PRV Becker and, vice versa, that infectious virus titers observed for PRV158 at 8 hpi were significantly lower than those observed for Bartha. In line with this, the addition of the corresponding supernatants to pDC-enriched PBMC showed that the IFN-α response induced by the supernatant from BaBe-infected cells was significantly increased compared to the response triggered by the supernatant from Becker-infected cells and vice versa for PRV158 and Bartha (Fig. 6D). Altogether, these results indicate that the US deletion in the Bartha genome plays critical roles in the increased virus titers observed in epithelial cells infected with the PRV strain Bartha and the concomitantly increased pDC response.

Next, using isogenic Becker deletion mutants lacking either US7 (gI) and US8 (gE), US9, or US2, the effects of the different genes affected by the US deletion on viral titers early in infection and the corresponding pDC IFN-α responses were assessed. As gE and gI form a heterodimer, and deletion phenotypes are generally interchangeable (13, 20, 21, 31, 52), a deletion mutant that encompasses both genes was used in these studies. As shown in Fig. 6E, the deletion of either US2 or gE/gI led to significantly increased virus titers at 8 hpi compared to the titers observed for the WT PRV Becker strain, similar to the increase observed using the BaBe strain (Becker strain with the Bartha US deletion). Correspondingly, pDC-enriched PBMC stimulated with the supernatant from cells infected with US2- or gE/gI-deleted Becker displayed a strongly increased IFN-α response, again similar to that when the supernatant of BaBe-infected cells was used (Fig. 6F). Again, we assessed whether these observations are reproducible using primary PK cells. In line with our above-described observations, the results were reproducible in primary epithelial cells, as infection of PK cells with PRV strains carrying a deletion in the US2 or gE/gI gene also led to increased viral titers (Fig. 6G) and concomitantly elevated IFN-α responses by pDC (Fig. 6H). In summary, the deletion of both US2 and gE/gI causes increased production of extracellular infectious virus early in infection of epithelial cells, which in turn leads to increased IFN-α responses by pDC.

Deletion of gE/gI significantly suppresses PRV L-particle production. Since Bartha-infected cells generate not only increased production of extracellular infectious virus early in infection but also reduced production of L-particles (Fig. 5), we next investigated whether the increased production of extracellular infectious virus observed upon the deletion of US2 or gE/gI also coincides with diminished L-particle production. To assess this, ST cells were infected with Becker WT, Becker US2null, Becker gE/gInull, or Becker US9null and examined by TEM at 12 hpi. Figure 7 shows that cells infected with Becker WT display substantial L-particle production, whereas L-particle production by cells infected with gE/gI-deleted Becker was almost completely abrogated. US2null PRV and, to a lesser extent, US9null PRV displayed a non-statistically significant trend of reduced L-particle production. These observations suggest that the expression of gE/gI not only suppresses the production of extracellular infectious virus but also stimulates the production of L-particles in infected epithelial cells.

FIG 6 Legend (Continued)
strains (MOI of 10) for 2 h, after which the cells were washed and overlaid with pDC medium. The supernatant was collected at 8 hpi and titrated (A, C, and E) or added to pDC-enriched PBMC populations for 22 h, after which IFN-α production was measured via an ELISA (B, D, and F). The viral titers shown represent average values $\pm$ standard deviations from four independent repeats. (G and H) Confluent primary PK cells were mock inoculated or inoculated with different PRV strains (MOI of 10) for 2 h, after which the cells were washed and overlaid with pDC medium. The supernatant was collected at 8 hpi and titrated (G) or added to pDC-enriched PBMC populations for 22 h, after which IFN-α production was measured via an ELISA (H) (ns, not significant; *, $P < 0.05$; **, $P < 0.01$; ***, $P < 0.001$).

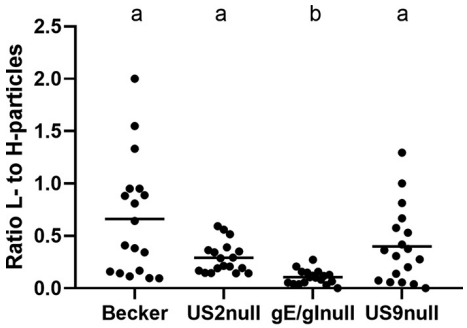

FIG 7 Deletion of the gE/gI genes results in significantly reduced production of noninfectious L-particles in PRV-infected ST cells at 12 hpi. Quantification of the L-to-H-particle ratios as determined by electron microscopy of ST cells 12 h after inoculation with WT PRV strain Becker or its isogenic US2null, gE/gInull, or US9null mutant strain are shown. Significantly different conditions are marked with different letters.

DISCUSSION

In the current report, we demonstrate that epithelial cells infected with the attenuated Bartha PRV vaccine strain elicit strongly increased IFN-α, IL-12/23, and TNF-α, but not IL-6, responses by primary porcine pDC compared to cells infected with wild-type (WT) PRV strains. Although pDC represent a minor fraction of PBMC, we found that these cells are major producers in the PBMC population with regard to these PRV-triggered cytokine responses. Moreover, quite surprisingly, we found that Bartha PRV replication in epithelial cells results in the faster production and release of infectious virus particles than with WT PRV and that this in turn leads to an elevated cytokine response by pDC. Despite this increased production of extracellular infectious virus, we confirm that the Bartha strain is attenuated in its ability to spread from cell to cell, as it causes reduced plaque sizes in cell monolayers. We show that the increased infectious virus production is not associated with augmented viral protein production or genome replication but does correlate with reduced production of L-particles. Using different PRV mutant strains, we show that the US deletion in Bartha, and particularly the deletion of the genes encoding US2 and gE/gI, is responsible for the observed increase in the pDC response by increasing H-particle production, whereas the deletion of gE/gI leads to a severe reduction in L-particle formation.

pDC represent only 0.2 to 0.5% of the PBMC population, yet we and others showed that they are by far the major producers of type I IFNs in response to several herpesviruses, including PRV (37), HSV-1 (36), and human cytomegalovirus (HCMV) (53). Here, we have found that in response to PRV infection, pDC are also important producers of other proinflammatory cytokines, including IL-12/23 and TNF-α, in the PBMC population but do not produce detectable amounts of IL-6 in response to PRV-infected cells. The latter observation is in line with other research indicating that different signaling axes regulate the production of different cytokines by pDC (34). For example, whereas the nuclear translocation of the transcription factors IFN regulatory factor 5 (IRF-5) and NF-κB subunit p50 drives the expression of type I IFN in human pDC, the nuclear translocation of IRF-5, NF-κB p50, as well as NF-κB p65 is needed to drive the expression of IL-6 (54). It will therefore be interesting to assess in future assays the exact signaling axes triggered by PRV in pDC that may explain the observed lack of IL-6 induction. It is also of interest that although at later time points postinfection, the supernatant of WT PRV-infected epithelial cells contains sufficient virus particles to stimulate pDC (Fig. 3C), pDC that have been in contact with WT PRV-infected epithelial cells from 2 hpi to 24 hpi still produce very little interferon or other cytokines (Fig. 1A). This suggests that factors present in or on PRV-infected epithelial cells suppress pDC activation at these stages of infection, a hypothesis that will be addressed in further research.

As an important sidenote, some care must be taken not to attribute pDC as the sole producers of IL-12/23 and TNF-α in response to PRV in the PBMC population, as our assays

employed pDC-enriched PBMC, which are to a substantial extent depleted of monocytes, a cell population known to also produce these cytokines upon stimulation (55).

Our observations here are in line with previous results regarding the cytokine response to Bartha PRV in mice. Laval and colleagues demonstrated that Bartha PRV, but not Becker WT PRV, induces high IFN-β titers at early time points of infection in mice (56). Moreover, it was established that one of the main reasons for mice succumbing to WT PRV infection is severe systemic inflammation marked by the strong upregulation of IL-6 and granulocyte colony-stimulating factor (G-CSF), which was not observed during Bartha infection (57). This matches our observations here as Bartha-infected cells triggered pDC to produce large quantities of several immunostimulatory cytokines but not IL-6.

Although it is known that Bartha PRV has been generated by serial passaging in cell culture, details regarding the origin, passaging method, or utilized cell line(s) are unclear (5). Our results contribute to the idea that the method for the generation of the Bartha vaccine strain has resulted in the impaired ability of the virus to suppress the production and antiviral activities of type I interferon. Indeed, brain tissue of Bartha-infected rats shows a strong upregulation of interferon-induced genes (58), and Bartha-infected rat fibroblasts have an enhanced sensitivity to type I interferon compared to WT PRV due to reduced interference with STAT1 phosphorylation (59). Our current data add to this idea and suggest that cell culture passage of the virus, in the absence of immune effectors like pDC, may have resulted in an evolutionary path toward decreased production of extracellular noninfectious L-particles that may suppress the immune response and increased extracellular production of bona fide virions (H-particles), which is associated with increased pDC activation. In line with this, we showed recently that the presence of L-particles suppresses the ability of PRV to activate pDC (37).

Using isogenic knockout mutants, we found that both US2 and gE/gI regulate extracellular viral titers by suppressing H-particle formation. In accordance, it was demonstrated previously that the deletion of gE provides a growth advantage for PRV in chicken embryo fibroblast (CEF) cells but not rabbit kidney (RK) cells (13, 51). It is likely that the advantages of gE deletion with regard to virus growth in cell culture may depend on the cell type and host species. Such differences may explain why the deletion of gE/gI from the PRV genome did not lead to higher extracellular viral titers in hamster BHK21 cells (60–63), and in contrast to our data here, Bartha was found to display impaired virus release in RK cells (25, 52, 64, 65).

For HSV-1, gE has been reported previously to play a pivotal role in the sorting and release of nascent virus in polarized epithelial cells (66, 67). Under these circumstances, gE drives the transport of newly assembled viral particles to the basolateral cell junctions. In the absence of gE, basolateral sorting is abrogated, and nascent virions are predominantly transported to the apical side in the supernatant. As a result, extracellular viral titers of HSV-1 gEnull have been observed to increase faster than those of WT HSV-1 (66). In addition, others also observed the enhanced release of HSV-1 gEnull virions in nonpolarized Vero cells (68, 69). Our current data indicate that the increased production of cell-free virus by infected epithelial cells in the absence of gE is conserved in different alphaherpesviruses, including HSV-1 and PRV.

Although until recently, US2 deletion had not been formally correlated with the increased production of cell-free virus, curiously, several indications for such a correlation can be found in the literature, where the data shown indicated that US2null virus displayed increased production of cell-free infectious virus without formally noting this observation (15, 29, 30). Only recently was it reported that the deletion of US2 resulted in increased virus titers (and increased viral genome production) at the early stages of infection in primary porcine cerebral cortex tissue (70). In any case, different independent studies suggest that the deletion of US2 (and gE) may have a beneficial effect on virus growth in cell culture. For example, in addition to Bartha PRV, the attenuated BUK strain, which was also obtained by serial passaging (49, 50), harbors a similar large US

deletion that also affects US2 and gE, in combination with US9 (47, 51). In line with our data on the Bartha strain, we observed that the BUK strain also displayed increased production of extracellular infectious virus early in infection and triggered increased IFN-α production by pDC, compared to WT PRV (Fig. 6A and B). Moreover, serial passaging of the recent virulent Chinese PRV strain JS-2012 on Vero cells similarly resulted in the deletion of US2 together with gE and US9. Interestingly, in line with the current results, the passage mutant JS-2012-F120 exhibited increased viral titers in the cell supernatant compared to the parental strain (71). Finally, independent serial passaging of PRV UL31null and UL34null mutants in order to regain replication competence also resulted in US2 deletion in both strains (72). In the former, US9, gE, and gI were also removed, while in the latter, the gI gene was deleted in addition to US2. Clearly, there appears to be a strong growth advantage for US2 and gE deletion when growing PRV in several cell culture systems. Interestingly, US9 often appears to be deleted in conjunction with gE and US2, yet our data showed no apparent growth advantage in epithelial cell cultures upon deletion. Although speculative at this point, its location between US8 (gE) and US2 may indicate that the removal of US9 could be a bystander deletion. While this deletion does not appear to have any particular advantage or disadvantage with regard to virus growth in epithelial cell cultures, neuronal anterograde transport of a US9null virus is abolished, thereby leading to severe attenuation *in vivo* (73, 74).

How the deletion of gE/gI leads to a decrease in L-particle formation remains to be investigated. Previous research has indicated that the cytoplasmic domain of gE that interacts with several tegument proteins (22, 23, 75) is a crucial component of the protein-protein interaction spectrum that leads to virus budding at membranes derived from the *trans*-Golgi network and is also involved in creating L-particles.

It is curious that PRV strains that are passaged through cell cultures tend to favor mutations that lead to the rapid production of extracellular virions, as this is in contrast to one of the main *in vivo* characteristics of alphaherpesviruses, i.e., their nature as cell-associated viruses that are highly proficient in cell-to-cell spread (1, 76, 77). The latter includes a variety of mechanisms of intercellular spread, including via cell-cell fusion (78), tunneling nanotubes (79), or intercellular junctions (66). As a result of cell-associated spread, herpesviruses are thought to evade a variety of immune responses, including opsonizing antibodies, complement factors, and immune cells (80, 81). During passaging in cell culture, the acquisition of mutations promoting the rapid release of viral progeny may allow these virions to (more rapidly) infect naive cells at greater distances in the cell culture than through classical cell-cell spread, thereby likely outcompeting ancestral strains. Although speculative at this point, as a consequence, progeny virus may simultaneously and gradually lose immune evasion mechanisms, which may, in turn, contribute to the potent antiviral responses elicited by cell culture-passaged attenuated PRV strains like the Bartha or BUK strain (5, 49). With the current study, we propose that the deletion of US2 and/or gE/gI provides an advantage to PRV with regard to the efficient production of cell-free virus in cell culture and that this comes at the expense of eliciting an increased antiviral response by pDC.

MATERIALS AND METHODS

Cells and viruses. Swine testis (ST) cells were cultured in minimum essential medium (MEM) with 10% fetal calf serum (FCS), 1 mM sodium pyruvate, and antibiotics (100 U/mL penicillin, 0.1 mg/mL streptomycin, and 0.05 mg/mL gentamicin) (all from Life Technologies). Primary porcine kidney (PK) cells were cultured in MEM with 10% FCS, 2 mM L-glutamine, 0.5% (wt/vol) lactalbumin lysate (BD), and antibiotics. All PBMC-derived populations were cultured in pDC medium, containing RPMI 1640 (Life Technologies) with 10% FCS, 2 mM L-glutamine, 1 mM sodium pyruvate, 1 mM nonessential amino acids, 20 μM β-mercaptoethanol (Sigma), and antibiotics.

All viruses utilized in the current study have been described previously: Becker WT (82), Kaplan WT (83), Bartha (5), PRV158 (Bartha with the large US deletion repaired) (84), BaBe (Becker with the large Bartha US deletion introduced) (14), PRV99 (isogenic gE- and gI-deleted Becker) (20), PRV161 (isogenic US9-deleted Becker) (16), and PRV174 (isogenic US2-deleted Becker) (29). Becker PRV and the derived mutant strains, including PRV158, were a kind gift from L. Enquist (Princeton University, USA); Kaplan

PRV was kindly donated by T. Mettenleiter (Friedrich Loeffler Institut, Germany); and Bartha and BUK PRV vaccine strains were kindly donated by H. Nauwynck (Ghent University, Belgium).

Antibodies and reagents. Antibodies for flow cytometry and Western blotting against the PRV glycoproteins gB (clone 1C11) (monoclonal IgG2a), gD (clone 13D12) (mIgG1), and gE (clone 18E8) (mIgG1) have been described previously (85). The antibodies against VP5 (clone 3C10) and US3 (clone 8F86) (mIgG1) (86) were kindly provided by L. Enquist (Princeton University, USA). The polyclonal anti-PRV IE180 serum was a kind gift from E. Tabares (Universidad Autónoma de Madrid, Spain) (87). Horseradish peroxidase (HRP)-conjugated antibodies against tubulin were obtained from Abcam (catalog number Ab40742), and HRP-conjugated goat anti-mouse IgG was purchased from Dako (catalog number P0447). Alexa Fluor 488-conjugated goat anti-mouse IgG (catalog number A-11029) was obtained from Life Technologies, and propidium iodide (PI) was purchased from Invitrogen (catalog number P3566). For magnetically activated cell sorting (MACS) and fluorescence-activated cell sorting (FACS), antibodies directed against CD4 (clone 74-12-4) (mIgG2b) (88) and CD172a (clone 74-33-15) (mIgG1) (88) were utilized and were kindly donated by A. Saalmüller (University of Vienna, Austria), and the mouse anti-CD14 antibodies (clone MIL-2) (mIgG2b) (89) were a kind gift from K. Haverson (Bristol University, UK). Alexa Fluor 647-labeled goat anti-mouse IgG1 (catalog number A21240), Alexa Fluor 488-conjugated goat anti-mouse IgG1 (catalog number A21121), phycoerythrin (PE)-labeled streptavidin (catalog number SA10041), and Sytox blue live/dead marker (catalog number S34857) were purchased from Life Technologies. MACS anti-mouse IgG (catalog number 130-048-401) and anti-mouse IgG1 microbeads (catalog number 130-047-101) were purchased from Miltenyi Biotec. For enzyme-linked immunosorbent assays (ELISAs), the porcine IFN-α antibodies F17 and K9 (both mIgG1) were a kind gift from B. Charley (INRA, France) (90). Recombinant porcine IFN-α was obtained from PBL Assay Science (catalog number 17105-1), streptavidin-HRP was obtained from Thermo Scientific (catalog number N100), bovine serum albumin (BSA) (fraction V) was obtained from Sigma-Aldrich (catalog number 1120180100), and 3,3′,5,5′-tetramethylbenzidine one-component substrate was obtained from Bethyl Laboratories (catalog number E102). Antibodies against CD4 and IFN-α (K9) were biotinylated using EZ-Link sulfo-N-hydroxysulfosuccinimide-biotin (sulfo-NHS-biotin, Life Technologies) according to the manufacturer's instructions. The type A CpG D32 (91) was synthesized by Integrated DNA Technologies.

PBMC isolation, pDC enrichment, and purification. Porcine PBMC isolation, pDC enrichment, purification, and depletion were performed as described previously (37).

Primary PK cell isolation. Primary porcine kidney cells were isolated as described previously (92).

Interferon assays. For IFN assays including infected ST or primary PK cells, cells were mock infected or infected with PRV (multiplicity of infection [MOI] of 10) for 2 h in MEM at 37°C, and 2 h later, cells were washed three times with MEM, followed by the addition of pDC medium. If appropriate, a positive-control condition including 10 μg/mL CpG ODN D32 was included. Unless mentioned otherwise, 800,000 pDC-enriched PBMC per mL were added for 22 h, after which the supernatant was collected and stored at −80°C until further analysis. For IFN assays without infected ST cells, i.e., cell-free assays, ST cells were mock infected or infected with PRV (MOI of 10) for 2 h in MEM at 37°C, and 2 h later, cells were washed three times with MEM, followed by the addition of pDC medium. The supernatant containing the extracellular virions was collected at the indicated time points, centrifuged for 10 min at 1,000 $\times$ *g*, and added at 1:2 to 800,000 pDC-enriched PBMC per mL for 22 h, after which the supernatant was collected and stored at −80°C until further analysis.

Ultracentrifugation. For the linear density purification of infectious Bartha and Kaplan virions, ultracentrifugation assays were performed as described previously (37). Briefly, 175-cm^2 flasks with confluent ST cells were inoculated with WT Kaplan or Bartha PRV (MOI of 10) in MEM at 37°C. At 2 hpi, virions that did not enter into a host cell (nonentered virions) were inactivated by citrate treatment for 2 min (40 mM sodium citrate, 10 mM KCl, 135 mM NaCl [pH 3]), after which the cells were washed two times and overlaid with ST medium. The supernatant was collected at 24 hpi, and cell debris was removed by centrifugation for 10 min at 1,000 $\times$ *g* and a 0.45-μm filtration step. Virions were pelleted for 1 h at 20,000 $\times$ *g* using a type 35 rotor (Beckman Coulter), resuspended in phosphate-buffered saline (PBS), briefly sonicated, carefully layered onto a 30 to 10% iodixanol (Sigma) gradient, and centrifuged for 2 h at 68,400 $\times$ *g* in an SW41-Ti rotor (Beckman Coulter). The bands containing the infectious virions were collected, aliquoted, and stored at −80°C until further use. For the depletion of infectious Bartha or Kaplan virions, ST cells were infected analogously, and the supernatant was collected at 8 hpi, after which it was centrifuged for 10 min at 1,000 $\times$ *g* to remove cell debris and virions were subsequently removed by centrifugation for 3 h at 100,000 $\times$ *g* using an SW41-Ti rotor (Beckman Coulter).

ELISA. The porcine IFN-α titers were determined by an ELISA as described previously (37). Quantification of porcine IL-6, IL-12/23 p40, and TNF-α was performed with the appropriate DuoSet ELISA kit according to the manufacturer's instructions (catalog numbers DY686, DY912, and DY690B, respectively; R&D).

Plaque size determination. ST cells were infected (MOI of 0.001) for 2 h in MEM at 37°C, after which nonentered virions were inactivated with citrate buffer for 2 min (40 mM sodium citrate, 10 mM KCl, 135 mM NaCl [pH 3]). Cells were subsequently washed and overlaid with ST medium containing 1% carboxymethyl cellulose to prevent secondary plaques. At 24 hpi, cells were fixed with 3% paraformaldehyde in PBS and permeabilized with 0.1% Triton X-100, and infected cells were visualized by staining the viral proteins gB and gD. Plaques were determined by fluorescence microscopy (Leica), and sizes were calculated with FIJI ImageJ.

Flow cytometry. Confluent ST cells were mock or PRV infected (MOI of 10) for 2 h in MEM at 37°C, after which the virus inoculum was removed, and cells were washed three times and overlaid with ST medium. ST cells were detached at 24 hpi with Accutase (BioLegend) and stained for gB and gE. Briefly, cells were incubated with primary antibodies for 30 min at 4°C, washed three times, incubated for 30 min at 4°C with secondary antibodies and PI (1/1,000), and analyzed by flow cytometry (Novocyte; ACEA).

Western blot analysis. ST cells were mock or PRV infected (MOI of 10) in MEM at 37°C; at 2 hpi, the virus inoculum was removed; and the cells were washed and overlaid with ST medium. Cells were detached at 4, 8, and 12 hpi by scraping; collected; centrifuged; washed in PBS; and lysed in radioimmunoprecipitation assay (RIPA) lysis buffer (Abcam) plus a protease inhibitor cocktail (Sigma-Aldrich). Nuclei were removed by spinning at 10,000 × *g* for 10 min at 4°C, after which protein concentrations in the supernatant were determined using the Pierce bicinchoninic acid (BCA) kit according to the manufacturer's instructions (Thermo Fisher). Samples were heated for 5 min at 95°C in SDS-PAGE loading buffer with or without β-mercaptoethanol, and 20 μg protein was separated on 10% polyacrylamide gels by SDS-PAGE. Separated proteins were blotted onto a Hybond-P polyvinylidene difluoride (PVDF) membrane (GE Healthcare) and incubated in blocking buffer (PBS containing 5% milk powder [Nestlé] and 0.1% Tween 20 [Sigma-Aldrich]) for 1 h at room temperature. Blots were subsequently incubated with primary antibodies overnight in blocking buffer at 4°C, washed in PBS plus 0.1% Tween 20, and incubated with HRP-labeled secondary antibodies in blocking buffer for 1 h at room temperature. Blots were developed using chemiluminescence (GE Healthcare).

PRV genome quantification. ST cells were PRV infected (MOI of 10) for 2 h in MEM at 37°C, after which nonentered virions were inactivated with citrate buffer for 2 min (40 mM sodium citrate, 10 mM KCl, 135 mM NaCl [pH 3]). Cells were subsequently washed and overlaid with ST medium. Infected cells were detached by scraping and washed in PBS, and the DNA was extracted using the DNeasy minikit according to the manufacturer's instructions (Qiagen). qPCR amplifications were carried out with SYBR green PCR master mix (Thermo Fisher) according to the manufacturer's instructions. Primers were targeted against the viral US3 gene (forward primer 5′-GACGGGGGGTTTCCTGATTTA and reverse primer 5′-GTATCTCATCAGCGGAAGGGC) and the porcine beta-2-microglobulin gene as a normalization control (forward primer 5′-AAACGGAAAGCCAAATTACC and reverse primer 5′-ATCCACAGCGTTAGGAG TGA). To eliminate bias caused by the template, amplification efficiencies of the US3 primer set were verified against a 10-fold serial dilution of the Bartha and Kaplan template. Calibrated normalized relative genome copy numbers were calculated according to the method described previously by Hellemans et al. (93).

Single-step growth curve. ST cells were PRV infected (MOI of 10) for 2 h in MEM at 37°C, after which nonentered virions were inactivated with citrate buffer for 2 min (40 mM sodium citrate, 10 mM KCl, 135 mM NaCl [pH 3]). Cells were subsequently washed and overlaid with ST medium. For the extracellular virion titers, the supernatant was collected, centrifuged for 10 min at 1,000 × *g*, and stored at −80°C until titration. Next, the intracellular virions were collected by scraping the infected cells into fresh medium, pelleted by centrifugation, and resuspended in cold citrate buffer for 2 min, after which cold RPMI 1640 medium was added to neutralize the acidic pH. The cells were washed and frozen in volumes equal to those used for the extracellular titers. Intracellular virus was released by three −80°C freeze-thaw cycles and subsequently titrated.

Viral titer determination. The virus supernatant was serially 10-fold diluted in ST medium and overlaid onto confluent ST cells for 1 h. Subsequently, ST medium was added, and cells were incubated for 7 days at 37°C. Virus titers were calculated and expressed as 50% tissue culture infectious doses ($TCID_{50}$).

Transmission electron microscopy. ST cells were PRV infected (MOI of 10) for 2 h in MEM at 37°C, and 2 h later, cells were washed three times with prewarmed MEM and overlaid with prewarmed ST medium. At the indicated time points, infected cells were prepared for and analyzed by TEM, using a JEOL JEM-1400 Plus transmission electron microscope, as described previously (79). H-particles and L-particles were determined, and ratios were calculated. At least 500 viral particles were counted in a total of 16 to 18 different pictures for each strain at each time point.

Statistical analysis. Statistical analysis was performed using GraphPad Prism. IFN-α data were analyzed using Student's *t* test or repeated-measures analysis of variance (ANOVA) at the 5% significance level. For the latter, *post hoc* comparisons between different conditions were performed by Tukey's range test. Log_{10}-transformed virus titers were analyzed using Student's *t* test or ANOVA at the 5% significance level. When appropriate, the Holm-Sidak method was used to correct for multiple comparisons. ANOVA *post hoc* comparisons were performed using Tukey's range test.

ACKNOWLEDGMENTS

J.L.D. is supported by a Ph.D. grant from the Research Foundation Flanders (F.W.O.-Vlaanderen) (https://www.fwo.be). This research was supported by grants to H.W.F. from the F.W.O.-Vlaanderen (grant numbers G017615 and G.019617N) (https://www.fwo.be) and the Special Research Fund of Ghent University (G.O.A. grant 01G01317 and grant BOFBAS2018000301) (https://www.ugent.be). The funders had no role in study design, data collection and analysis, decision to publish, or preparation of the manuscript.

We thank Lynn Enquist (Princeton University, USA) for donating Becker WT, PRV158, PRV BaBe, PRV161, PRV174, PRV99, and the US3 and VP5 antibodies; Thomas Mettenleiter (Friedrich Loeffler Institut, Germany) for donating the Kaplan strain; Hans Nauwynck (Ghent University, Belgium) for donating the Bartha and BUK strains; A. Saalmüller (University of Vienna, Austria) for the CD172a antibodies; E. Tabares for the

IE180 antiserum; K. Haverson (Bristol University, UK) for the CD14 antibodies; and B. Charley (INRA, France) for the porcine IFN-α antibodies F17 and K9. We also thank Rudy Cooman and Jan Clement for animal caretaking.

REFERENCES

1. Pomeranz LE, Reynolds AE, Christoph J, Hengartner CJ. 2005. Molecular biology of pseudorabies virus: impact on neurovirology and veterinary medicine. Microbiol Mol Biol Rev 69:462–500. https://doi.org/10.1128/MMBR.69.3.462-500.2005.
2. Mettenleiter TC, Ehlers B, Müller T, Yoon K-J, Teifke JP. 2012. Viral diseases, herpesviruses, p 421–434. *In* Zimmerman JJ, Karriker LA, Ramirez A, Schwartz KJ, Stevenson GW (ed), Diseases of swine, 11th ed. John Wiley & Sons, Chichester, United Kingdom.
3. Liu Y, Chen Q, Rao X, Diao X, Yang L, Fang X, Hogeveen H. 2019. An economic assessment of pseudorabies (Aujeszky' disease) elimination on hog farms in China. Prev Vet Med 163:24–30. https://doi.org/10.1016/j.prevetmed.2018.12.005.
4. Freuling CM, Müller TF, Mettenleiter TC. 2017. Vaccines against pseudorabies virus (PrV). Vet Microbiol 206:3–9. https://doi.org/10.1016/j.vetmic.2016.11.019.
5. Bartha A. 1961. Experiments to reduce the virulence of Aujeskzy's virus. Magy Allatorvosok Lapja 16:42–45.
6. Delva JL, Nauwynck HJ, Mettenleiter TC, Favoreel HW. 2020. The attenuated pseudorabies virus vaccine strain Bartha K61: a brief review on the knowledge gathered during 60 years of research. Pathogens 9:897. https://doi.org/10.3390/pathogens9110897.
7. Szpara ML, Tafuri YR, Parsons L, Shamim SR, Verstrepen KJ, Legendre M, Enquist LW. 2011. A wide extent of inter-strain diversity in virulent and vaccine strains of alphaherpesviruses. PLoS Pathog 7:e1002282. https://doi.org/10.1371/journal.ppat.1002282.
8. Robbins AK, Ryan JP, Whealy ME, Enquist LW. 1989. The gene encoding the gIII envelope protein of pseudorabies virus vaccine strain Bartha contains a mutation affecting protein localization. J Virol 63:250–258. https://doi.org/10.1128/JVI.63.1.250-258.1989.
9. Schröter C, Klupp BG, Fuchs W, Gerhard M, Backovic M, Rey FA, Mettenleiter TC. 2014. The highly conserved proline at position 438 in pseudorabies virus gH is important for regulation of membrane fusion. J Virol 88:13064–13072. https://doi.org/10.1128/JVI.01204-14.
10. Klupp BG, Lomniczi B, Visser N, Fuchs W, Mettenleiter TC. 1995. Mutations affecting the UL21 gene contribute to avirulence of pseudorabies virus vaccine strain Bartha. Virology 212:466–473. https://doi.org/10.1006/viro.1995.1504.
11. Dijkstra JM, Mettenleiter TC, Klupp BG. 1997. Intracellular processing of pseudorabies virus glycoprotein M (gM): gM of strain Bartha lacks N-glycosylation. Virology 237:113–122. https://doi.org/10.1006/viro.1997.8766.
12. Lomniczi B, Watanabe S, Ben-Porat T, Kaplan AS. 1984. Genetic basis of the neurovirulence of pseudorabies virus. J Virol 52:198–205. https://doi.org/10.1128/JVI.52.1.198-205.1984.
13. Zuckermann FA, Mettenleiter TC, Schreurs C, Sugg N, Ben-Porat T. 1988. Complex between glycoproteins gI and gp63 of pseudorabies virus: its effect on virus replication. J Virol 62:4622–4626. https://doi.org/10.1128/JVI.62.12.4622-4626.1988.
14. Card J, Whealy M, Robbins A, Enquist L. 1992. Pseudorabies virus envelope glycoprotein gI influences both neurotropism and virulence during infection of the rat visual system. J Virol 66:3032–3041. https://doi.org/10.1128/JVI.66.5.3032-3041.1992.
15. Kratchmarov R, Kramer T, Greco TM, Taylor MP, Hean T, Cristea IM, Enquist LW. 2013. Glycoproteins gE and gI are required for efficient KIF1A-dependent anterograde axonal transport of alphaherpesvirus particles in neurons. J Virol 87:9431–9440. https://doi.org/10.1128/JVI.01317-13.
16. Brideau AD, Card JP, Enquist LW. 2000. Role of pseudorabies virus Us9, a type II membrane protein, in infection of tissue culture cells and the rat nervous system. J Virol 74:834–845. https://doi.org/10.1128/jvi.74.2.834-845.2000.
17. Ch'ng TH, Enquist LW. 2005. Neuron-to-cell spread of pseudorabies virus in a compartmented neuronal culture system. J Virol 79:10875–10889. https://doi.org/10.1128/JVI.79.17.10875-10889.2005.
18. Husak PJ, Kuo T, Enquist LW. 2000. Pseudorabies virus membrane proteins gI and gE facilitate anterograde spread of infection in projection-specific neurons in the rat. J Virol 74:10975–10983. https://doi.org/10.1128/jvi.74.23.10975-10983.2000.
19. Mulder WAM, Jacobs L, Priem J, Kok GL, Wagenaar F, Kimman TG, Pol JMA. 1994. Glycoprotein gE-negative pseudorabies virus has a reduced capability to infect second- and third-order neurons of the olfactory and trigeminal routes in the porcine central nervous system. J Gen Virol 75:3095–3106. https://doi.org/10.1099/0022-1317-75-11-3095.
20. Whealy ME, Card JP, Robbins AK, Dubin JR, Rziha HJ, Enquist LW. 1993. Specific pseudorabies virus infection of the rat visual system requires both gI and gp63 glycoproteins. J Virol 67:3786–3797. https://doi.org/10.1128/JVI.67.7.3786-3797.1993.
21. Tirabassi RS, Enquist LW. 2000. Role of the pseudorabies virus gI cytoplasmic domain in neuroinvasion, virulence, and posttranslational N-linked glycosylation. J Virol 74:3505–3516. https://doi.org/10.1128/jvi.74.8.3505-3516.2000.
22. Brack AR, Klupp BG, Granzow H, Tirabassi R, Enquist LW, Mettenleiter TC. 2000. Role of the cytoplasmic tail of pseudorabies virus glycoprotein E in virion formation. J Virol 74:4004–4016. https://doi.org/10.1128/jvi.74.9.4004-4016.2000.
23. Fuchs W, Klupp BG, Granzow H, Hengartner C, Brack A, Mundt A, Enquist LW, Mettenleiter TC. 2002. Physical interaction between envelope glycoproteins E and M of pseudorabies virus and the major tegument protein UL49. J Virol 76:8208–8217. https://doi.org/10.1128/jvi.76.16.8208-8217.2002.
24. Brack AR, Dijkstra JM, Granzow H, Klupp BG, Mettenleiter TC. 1999. Inhibition of virion maturation by simultaneous deletion of glycoproteins E, I, and M of pseudorabies virus. J Virol 73:5364–5372. https://doi.org/10.1128/JVI.73.7.5364-5372.1999.
25. Ben-Porat T, Demarchi J, Pendrys J, Veach RA, Kaplan AS. 1986. Proteins specified by the short unique region of the genome of pseudorabies virus play a role in the release of virions from certain cells. J Virol 57:191–196. https://doi.org/10.1128/JVI.57.1.191-196.1986.
26. Lamote JAS, Kestens M, Van Waesberghe C, Delva J, De Pelsmaeker S, Devriendt B, Favoreel HW. 2017. The pseudorabies virus glycoprotein gE/gI complex suppresses type I interferon production by plasmacytoid dendritic cells. J Virol 91:e02276-16. https://doi.org/10.1128/JVI.02276-16.
27. Van Zijl M, Van Der Gulden H, De Wind N, Gielkens A, Berns A. 1990. Identification of two genes in the unique short region of pseudorabies virus; comparison with herpes simplex virus and varicella-zoster virus. J Gen Virol 71:1747–1755. https://doi.org/10.1099/0022-1317-71-8-1747.
28. Kang M-H, Banfield BW. 2010. Pseudorabies virus tegument protein Us2 recruits the mitogen-activated protein kinase extracellular-regulated kinase (ERK) to membranes through interaction with the ERK common docking domain. J Virol 84:8398–8408. https://doi.org/10.1128/JVI.00794-10.
29. Clase AC, Lyman MG, Rio T, Randall JA, Calton CM, Enquist LW, Banfield BW. 2003. The pseudorabies virus Us2 protein, a virion tegument component, is prenylated in infected cells. J Virol 77:12285–12298. https://doi.org/10.1128/jvi.77.22.12285-12298.2003.
30. Lyman MG, Randall JA, Calton CM, Banfield BW. 2006. Localization of ERK/MAP kinase is regulated by the alphaherpesvirus tegument protein Us2. J Virol 80:7159–7168. https://doi.org/10.1128/JVI.00592-06.
31. Mettenleiter TC, Zsak L, Kaplan AS, Ben-Porat T, Lomniczi B. 1987. Role of a structural glycoprotein of pseudorabies in virus virulence. J Virol 61:4030–4032. https://doi.org/10.1128/JVI.61.12.4030-4032.1987.
32. Kimman TG, De Wind N, Oei-Lie N, Pol JMA, Berns AJM, Gielkens ALJ. 1992. Contribution of single genes within the unique short region of Aujeszky's disease virus (suid herpesvirus type 1) to virulence, pathogenesis and immunogenicity. J Gen Virol 73:243–251. https://doi.org/10.1099/0022-1317-73-2-243.
33. Tang Y-D, Liu J-T, Wang T-Y, Sun M-X, Tian Z-J, Cai X-H. 2017. Comparison of pathogenicity-related genes in the current pseudorabies virus outbreak in China. Sci Rep 7:7783. https://doi.org/10.1038/s41598-017-08269-3.
34. Swiecki M, Colonna M. 2015. The multifaceted biology of plasmacytoid dendritic cells. Nat Rev Immunol 15:471–485. https://doi.org/10.1038/nri3865.
35. Liu Y-J. 2005. IPC: professional type 1 interferon-producing cells and plasmacytoid dendritic cell precursors. Annu Rev Immunol 23:275–306. https://doi.org/10.1146/annurev.immunol.23.021704.115633.
36. Siegal FP, Kadowaki N, Shodell M, Fitzgerald-Bocarsly P, Shah K, Ho S, Antonenko S, Liu YJ. 1999. The nature of the principal type 1 interferon-

producing cells in human blood. Science 284:1835–1837. https://doi.org/10.1126/science.284.5421.1835.
37. Delva JL, Van Waesberghe C, Klupp BG, Mettenleiter TC, Favoreel HW. 2021. Alphaherpesvirus-induced activation of plasmacytoid dendritic cells depends on the viral glycoprotein gD and is inhibited by non-infectious light particles. PLoS Pathog 17:e1010117. https://doi.org/10.1371/journal.ppat.1010117.
38. Baranek T, Zucchini N, Dalod M. 2009. Plasmacytoid dendritic cells and the control of herpesvirus infections. Viruses 1:383–419. https://doi.org/10.3390/v1030383.
39. Casrouge A, Zhang SY, Eidenschenk C, Jouanguy E, Puel A, Yang K, Alcais A, Picard C, Mahfoufi N, Nicolas N, Lorenzo L, Plancoulaine S, Senechal B, Geissmann F, Tabeta K, Hoebe K, Du X, Miller RL, Heron B, Mignot C, de Villemeur TB, Lebon P, Dulac O, Rozenberg F, Beutler B, Tardieu M, Abel L, Casanova JL. 2006. Herpes simplex virus encephalitis in human UNC-93B deficiency. Science 314:308–312. https://doi.org/10.1126/science.1128346.
40. Donaghy H, Bosnjak L, Harman AN, Marsden V, Tyring SK, Meng T-C, Cunningham AL. 2009. Role for plasmacytoid dendritic cells in the immune control of recurrent human herpes simplex virus infection. J Virol 83:1952–1961. https://doi.org/10.1128/JVI.01578-08.
41. Kittan NA, Bergua A, Haupt S, Donhauser N, Schuster P, Korn K, Harrer T, Schmidt B. 2007. Impaired plasmacytoid dendritic cell innate immune responses in patients with herpes virus-associated acute retinal necrosis. J Immunol 179:4219–4230. https://doi.org/10.4049/jimmunol.179.6.4219.
42. Dalloul A, Oksenhendler E, Chosidow O, Ribaud P, Carcelain G, Louvet S, Massip P, Lebon P, Autran B. 2004. Severe herpes virus (HSV-2) infection in two patients with myelodysplasia and undetectable NK cells and plasmacytoid dendritic cells in the blood. J Clin Virol 30:329–336. https://doi.org/10.1016/j.jcv.2003.11.014.
43. Swiecki M, Wang Y, Gilfillan S, Colonna M. 2013. Plasmacytoid dendritic cells contribute to systemic but not local antiviral responses to HSV infections. PLoS Pathog 9:e1003728. https://doi.org/10.1371/journal.ppat.1003728.
44. Villadangos A, Young L. 2008. Antigen-presentation properties of plasmacytoid dendritic cells. Immunity 29:352–361. https://doi.org/10.1016/j.immuni.2008.09.002.
45. Cella M, Facchetti F, Lanzavecchia A, Colonna M. 2000. Plasmacytoid dendritic cells activated by influenza virus and CD40L drive a potent TH1 polarization. Nat Immunol 1:305–310. https://doi.org/10.1038/79747.
46. Yoneyama H, Matsuno K, Toda E, Nishiwaki T, Matsuo N, Nakano A, Narumi S, Lu B, Gerard C, Ishikawa S, Matsushima K. 2005. Plasmacytoid DCs help lymph node DCs to induce anti-HSV CTLs. J Exp Med 202:425–435. https://doi.org/10.1084/jem.20041961.
47. Petrovskis EA, Timmins JG, Gierman TM, Post LE. 1986. Deletions in vaccine strains of pseudorabies virus and their effect on synthesis of glycoprotein gp63. J Virol 60:1166–1169. https://doi.org/10.1128/JVI.60.3.1166-1169.1986.
48. Heilingloh CS, Krawczyk A. 2017. Role of L-particles during herpes simplex virus infection. Front Microbiol 8:2565. https://doi.org/10.3389/fmicb.2017.02565.
49. Skoda R, Brauner I, Sadecky E, Mayer V. 1964. Immunization against Aujeszky's disease with live vaccine. I. Attenuation of virus and some properties of attenuated strains. Acta Virol 8:1–9.
50. Skoda R, Brauner I, S'Adecky E, Somogyiova J. 1964. Immunization against Aujeszky's disease with live vaccine. II. Immunization of pigs under laboratory conditions. Acta Virol 8:123–134.
51. Mettenleiter TC, Lomniczi B, Sugg N, Schreurs C, Ben-Porat T. 1988. Host cell-specific growth advantage of pseudorabies virus with a deletion in the genome sequences encoding a structural glycoprotein. J Virol 62:12–19. https://doi.org/10.1128/JVI.62.1.12-19.1988.
52. Mettenleiter TC, Schreurs C, Zuckermann F, Ben-Porat T. 1987. Role of pseudorabies virus glycoprotein gI in virus release from infected cells. J Virol 61:2764–2769. https://doi.org/10.1128/JVI.61.9.2764-2769.1987.
53. Zucchini N, Bessou G, Robbins SH, Chasson L, Raper A, Crocker PR, Dalod M. 2008. Individual plasmacytoid dendritic cells are major contributors to the production of multiple innate cytokines in an organ-specific manner during viral infection. Int Immunol 20:45–56. https://doi.org/10.1093/intimm/dxm119.
54. Steinhagen F, McFarland AP, Rodriguez LG, Tewary P, Jarret A, Savan R, Klinman DM. 2013. IRF-5 and NF-κB p50 co-regulate IFN-β and IL-6 expression in TLR9-stimulated human plasmacytoid dendritic cells. Eur J Immunol 43:1896–1906. https://doi.org/10.1002/eji.201242792.
55. Shi C, Pamer EG. 2011. Monocyte recruitment during infection and inflammation. Nat Rev Immunol 11:762–774. https://doi.org/10.1038/nri3070.
56. Laval K, Van Cleemput J, Vernejoul JB, Enquist LW. 2019. Alphaherpesvirus infection of mice primes PNS neurons to an inflammatory state regulated by TLR2 and type I IFN signaling. PLoS Pathog 15:e1008087. https://doi.org/10.1371/journal.ppat.1008087.
57. Laval K, Vernejoul JB, Van Cleemput J, Koyuncu OO, Enquist LW. 2018. Virulent pseudorabies virus infection induces a specific and lethal systemic inflammatory response in mice. J Virol 92:e01614-18. https://doi.org/10.1128/JVI.01614-18.
58. Paulus C, Sollars PJ, Pickard GE, Enquist LW. 2006. Transcriptome signature of virulent and attenuated pseudorabies virus-infected rodent brain. J Virol 80:1773–1786. https://doi.org/10.1128/JVI.80.4.1773-1786.2006.
59. Brukman A, Enquist LW. 2006. Suppression of the interferon-mediated innate immune response by pseudorabies virus. J Virol 80:6345–6356. https://doi.org/10.1128/JVI.00554-06.
60. Li W, Zhuang D, Li H, Zhao M, Zhu E, Xie B, Chen J, Zhao M. 2021. Recombinant pseudorabies virus with gI/gE deletion generated by overlapping polymerase chain reaction and homologous recombination technology induces protection against the PRV variant PRV-GD2013. BMC Vet Res 17:164. https://doi.org/10.1186/s12917-021-02861-6.
61. Yin Y, Xu Z, Liu X, Li P, Yang F, Zhao J, Fan Y, Sun X, Zhu L. 2017. A live gI/gE-deleted pseudorabies virus (PRV) protects weaned piglets against lethal variant PRV challenge. Virus Genes 53:565–572. https://doi.org/10.1007/s11262-017-1454-y.
62. Li J, Fang K, Rong Z, Li X, Ren X, Hui M, Chen H, Li X, Qian P. 2020. Comparison of gE/gI- and TK/gE/gI-gene-deleted pseudorabies virus vaccines mediated by CRISPR/Cas9 and Cre/Lox systems. Viruses 12:369. https://doi.org/10.3390/v12040369.
63. Gu Z, Dong J, Wang J, Hou C, Sun H, Yang W, Bai J, Jiang P. 2015. A novel inactivated gE/gI deleted pseudorabies virus (PRV) vaccine completely protects pigs from an emerged variant PRV challenge. Virus Res 195:57–63. https://doi.org/10.1016/j.virusres.2014.09.003.
64. Schreurs C, Mettenleiter TC, Zuckermann F, Sugg N, Ben-Porat T. 1988. Glycoprotein gIII of pseudorabies virus is multifunctional. J Virol 62:2251–2257. https://doi.org/10.1128/JVI.62.7.2251-2257.1988.
65. Zsak L, Mettenleiter TC, Sugg N, Ben-Porat T. 1989. Release of pseudorabies virus from infected cells is controlled by several viral functions and is modulated by cellular components. J Virol 63:5475–5477. https://doi.org/10.1128/JVI.63.12.5475-5477.1989.
66. Johnson DC, Webb M, Wisner TW, Brunetti C. 2001. Herpes simplex virus gE/gI sorts nascent virions to epithelial cell junctions, promoting virus spread. J Virol 75:821–833. https://doi.org/10.1128/JVI.75.2.821-833.2001.
67. Farnsworth A, Goldsmith K, Johnson DC. 2003. Herpes simplex virus glycoproteins gD and gE/gI serve essential but redundant functions during acquisition of the virion envelope in the cytoplasm. J Virol 77:8481–8494. https://doi.org/10.1128/jvi.77.15.8481-8494.2003.
68. Feutz E, McLeland-Wieser H, Ma J, Roller RJ. 2019. Functional interactions between herpes simplex virus pUL51, pUL7 and gE reveal cell-specific mechanisms for epithelial cell-to-cell spread. Virology 537:84–96. https://doi.org/10.1016/j.virol.2019.08.014.
69. Mingo RM, Han J, Newcomb WW, Brown JC. 2012. Replication of herpes simplex virus: egress of progeny virus at specialized cell membrane sites. J Virol 86:7084–7097. https://doi.org/10.1128/JVI.00463-12.
70. Lyu C, Wang S, Sun M, Tang Y, Peng J, Tian Z, Cai X. 2018. Deletion of pseudorabies virus US2 gene enhances viral titers in a porcine cerebral cortex primary culture system. Virus Genes 54:406–413. https://doi.org/10.1007/s11262-018-1552-5.
71. Liang C, Tong W, Zheng H, Liu F, Wu J, Li G, Zhou E, Tong G. 2017. A high-temperature passaging attenuated pseudorabies vaccine protects piglets completely against emerging PRV variant. Res Vet Sci 112:109–115. https://doi.org/10.1016/j.rvsc.2017.02.008.
72. Grimm KS, Klupp BG, Granzow H, Muller FM, Fuchs W, Mettenleiter TC. 2012. Analysis of viral and cellular factors influencing herpesvirus-induced nuclear envelope breakdown. J Virol 86:6512–6521. https://doi.org/10.1128/JVI.00068-12.
73. Wilson DW. 2021. Motor skills: recruitment of kinesins, myosins and dynein during assembly and egress of alphaherpesviruses. Viruses 13:1622. https://doi.org/10.3390/v13081622.
74. Lyman MG, Curanovic D, Brideau AD, Enquist LW. 2008. Fusion of enhanced green fluorescent protein to the pseudorabies virus axonal sorting protein Us9 blocks anterograde spread of infection in mammalian neurons. J Virol 82:10308–10311. https://doi.org/10.1128/JVI.01204-08.
75. Owen DJ, Crump CM, Graham SC. 2015. Tegument assembly and secondary envelopment of alphaherpesviruses. Viruses 7:5084–5114. https://doi.org/10.3390/v7092861.
76. Johnson DC, Baines JD. 2011. Herpesviruses remodel host membranes for virus egress. Nat Rev Microbiol 9:382–394. https://doi.org/10.1038/nrmicro2559.

77. Nauwynck H, Glorieux S, Favoreel H, Pensaert M. 2007. Cell biological and molecular characteristics of pseudorabies virus infections in cell cultures and in pigs with emphasis on the respiratory tract. Vet Res 38:229–241. https://doi.org/10.1051/vetres:200661.
78. Peeters B, de Wind N, Hooisma M, Wagenaar F, Gielkens A, Moormann R. 1992. Pseudorabies virus envelope glycoproteins gp50 and gII are essential for virus penetration, but only gII is involved in membrane fusion. J Virol 66:894–905. https://doi.org/10.1128/JVI.66.2.894-905.1992.
79. Jansens RJJ, Van Den Broeck W, De Pelsmaeker S, Lamote JAS, Van Waesberghe C, Couck L, Favoreel HW. 2017. Pseudorabies virus US3-induced tunneling nanotubes contain stabilized microtubules, interact with neighboring cells via cadherins, and allow intercellular molecular communication. J Virol 91:e00749-17. https://doi.org/10.1128/JVI.00749-17.
80. Dingwell KS, Brunetti CR, Hendricks RL, Tang Q, Tang M, Rainbow AJ, Johnson DC. 1994. Herpes simplex virus glycoproteins E and I facilitate cell-to-cell spread in vivo and across junctions of cultured cells. J Virol 68:834–845. https://doi.org/10.1128/JVI.68.2.834-845.1994.
81. Corey L, Spear PG. 1986. Infections with herpes simplex viruses. N Engl J Med 314:749–757. https://doi.org/10.1056/NEJM198603203141205.
82. Becker C. 1967. On primary damage of autonomic ganglia following infection with herpes suis virus in different animal species. Experientia 23:209–210. https://doi.org/10.1007/BF02136291.
83. Kaplan A, Vatter A. 1959. A comparison of herpes simplex and pseudorabies viruses. Virology 7:394–407. https://doi.org/10.1016/0042-6822(59)90068-6.
84. Demmin GL, Clase AC, Randall JA, Enquist LW, Banfield BW. 2001. Insertions in the gG gene of pseudorabies virus reduce expression of the upstream Us3 protein and inhibit cell-to-cell spread of virus infection. J Virol 75:10856–10869. https://doi.org/10.1128/JVI.75.22.10856-10869.2001.
85. Nauwynck HJ, Pensaert MB. 1995. Effect of specific antibodies on the cell-associated spread of pseudorabies virus in monolayers of different cell types. Arch Virol 140:1137–1146. https://doi.org/10.1007/BF01315422.
86. Olsen LM, Ch'ng TH, Card JP, Enquist LW. 2006. Role of pseudorabies virus Us3 protein kinase during neuronal infection. J Virol 80:6387–6398. https://doi.org/10.1128/JVI.00352-06.
87. Gomez-Sabastian S, Tabares E. 2004. Negative regulation of herpes simplex virus type 1 ICP4 promoter by IE180 protein of pseudorabies virus. J Gen Virol 85:2125–2130. https://doi.org/10.1099/vir.0.80119-0.
88. Pescovitz M, Lunney J, Sachs D. 1984. Preparation and characterization of monoclonal antibodies reactive with porcine PBL. J Immunol 133:368–375.
89. Haverson K, Bailey M, Higgins VR, Bland PW, Stokes CR. 1994. Characterization of monoclonal antibodies specific for monocytes, macrophages and granulocytes from porcine peripheral blood and mucosal tissues. J Immunol Methods 170:233–245. https://doi.org/10.1016/0022-1759(94)90398-0.
90. L'Haridon RM, Bourget P, Lefevre F, La Bonnardiere C. 1991. Production of an hybridoma library to recombinant porcine alpha I interferon: a very sensitive assay (ISBBA) allows the detection of a large number of clones. Hybridoma 10:35–47. https://doi.org/10.1089/hyb.1991.10.35.
91. Guzylack-Piriou L, Balmelli C, McCullough KC, Summerfield A. 2004. Type-A CpG oligonucleotides activate exclusively porcine natural interferon-producing cells to secrete interferon-alpha, tumour necrosis factor-alpha and interleukin-12. Immunology 112:28–37. https://doi.org/10.1111/j.1365-2567.2004.01856.x.
92. Geenen K, Favoreel HW, Nauwynck HJ. 2005. Higher resistance of porcine trigeminal ganglion neurons towards pseudorabies virus-induced cell death compared with other porcine cell types in vitro. J Gen Virol 86:1251–1260. https://doi.org/10.1099/vir.0.80760-0.
93. Hellemans J, Mortier G, De Paepe A, Speleman F, Vandesompele J. 2007. qBase relative quantification framework and software for management and automated analysis of real-time quantitative PCR data. Genome Biol 8:R19. https://doi.org/10.1186/gb-2007-8-2-r19.